APPLICATION OF THE STEERABLE FILTERS FOR GRAVITY ANOMALY MAP OF HATAY REGION

Didem ERDOĞAN[1] Osman N. UÇAN[1] A. Muhittin ALBORA[2] and Atilla ÖZMEN[3]
e-mail: dideme@istanbul.edu.tr uosman@istanbul.edu.tr muhitin@istanbul.edu.tr aozmen@khas.edu.tr

[1]Istanbul University, Engineering Faculty, Electrical & Electronics Department, 34320, Avcilar, Istanbul, Turkey
[2]Istanbul University, Engineering Faculty, Geophysical Department, 34320, Avcilar, Istanbul, Turkey
[3] Kadir Has Üniversity, Engineering Faculty, Electronics Department, 34230 Cibali , Istanbul

Key words: Steerable filters, image process, gravity anomaly, fault

ABSTRACT

In this paper, Steerable Filters are used for the solutions of some problems in Geophysics. Steerable Filters are band pass filters that pass band in a contain direction. Different sides in an image are obtained after image is passed from fundamental filters and then separated to direction sub bands. In this study, Steerable filters are applied to synthetic data with various angles to determine the sides. As a field study gravity anomaly map of Hatay region is used. The anomalies caused by buried faults are found by Steerable Filters and fault map of the region are compared to Geological data.

I. INTRODUCTION

As one of the contemporary approaches, steerable filters have the directional property and the have been applied successfully among others, to biomedical data, hand-written character recognition, fault analysis, border detection. Steerable filters were first defined by [1], and then studied by many scientists such as [2], [3]. There are various approaches in the application of these filters. One approach is to apply many versions of the same steerable filter, each different from the others by some small rotation in angle. A more efficient approach is to apply a few filters corresponding to a few angles and interpolate between the results.

There are many researches on separation of potential anomalies and border detection of buried structures using wavelet approaches. [4] has first used the wavelet transform for potential-field data. Afterwards [5] have worked upon seismological data. [6] had separated regional and residual potential-field anomalies using the wavelet transform. [7] has separated potential anomaly data by wavelet approach. [8] processed aero magnetic data by the wavelet transform. [9] have modeled geometric of geological bodies using multiscale edge analysis and forward modeling based on wavelet. [10] have studied on de-noising of signals from potential field effects and tried to estimate borders of the buried objects. [11] have applied the wavelet transform to magnetic synthetic examples. [12] have also detected the borders of underground geological bodies using wavelet transform. [13], [14] have applied wavelet approach to archeological sites and estimated the borders of ancient cities.

In this paper, we use steerable filters in edge detection of the faults and their directions using gravity anomaly maps as input. We demonstrate the procedure on both synthetic and real data for Hatay region of Turkey and model the region regarding steerable filter outputs. The results are compared to results interred from geological studies. The comparison shows that a good agreement exists between various approaches.

II. MATHEMATICAL ANALYSIS

In geophysics, one of the main problems is to delineate the edges of the buried objects. The detection of borders of subsurface bodies can be investigated by using either derivative based classical approaches or contemporary image processing algorithms such as steerable filters. These filters with directional properties can be used in detection of the borders faults or other geometric structures such as walls of historical sites. Steerable filters were first defined by [1], and then studied by many scientists such as [2], [3]. In steerable filters, impulse function $h^{\theta_a}(x,y)$ of any arbitrary angle θ_a, can be expressed as a combination of basis functions $h^{\theta_i}(x,y)$, $i=1,..,M$ as [1],

$$h^{\theta_a}(x,y)=\sum_{i=1}^{M}k_i(\theta_a)h^{\theta_i}(x,y) \qquad (1)$$

where $k_i(\theta_a)$, $1 \le i \le M$, are the filter coefficients (Figure 1). Here, it is necessary to define which functions *h(x,y)* can satisfy Equation 1 and what are the interpolation functions $k_i(\theta)$. Let *h* be any function which can be expanded in a Fourier series in polar angle θ as,

$$h(r,\theta) = \sum_{n=-N}^{N} a_n(r) e^{jn\theta_a} \tag{2}$$

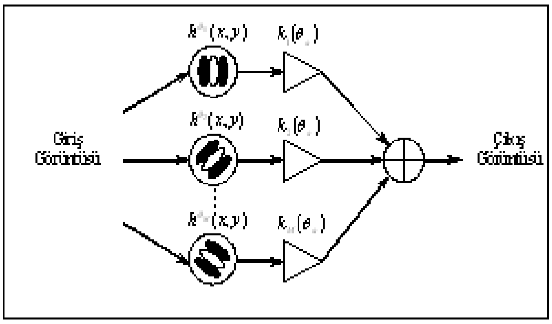

Figure 1. Block diagram of steerable filter.

where $r = \sqrt{x^2 + y^2}$ and $\theta = \arg(x,y)$ in polar coordinates. The steering condition (Equation 1), holds for functions expandable in the form of Equation (2) if and only if the interpolation functions $k_i(\theta)$ are the solutions of,

$$e^{jl\theta_a} = \sum_{i=1}^{M} e^{jl\theta_i} k_i(\theta_a), \qquad 0 \le l \le N \cdot \tag{3}$$

Thus any directed impulse response of the input data can be obtained by using Equations (1-3).

In steerable filtering, enhancement is achieved for any arbitrary direction of the input data, while minimising the other effects in other directions. Thus steerable filters are used in various areas such as pattern recognition and fault analysis. There are many $h(x,y)$ functions, which can be chosen as steering functions satisfying Equations (1-3). Here we have chosen the two-dimensional Gaussian function as impulse response, $h(x,y) = e^{-(x^2+y^2)/2}$. As basis functions, we have derived the Gaussian function at 0 and 90 degrees as follows,

$$h^0(x,y) = \frac{\partial}{\partial x} e^{-(x^2+y^2)/2} = -2xe^{-(x^2+y^2)/2} \tag{4}$$

$$h^{90}(x,y) = \frac{\partial}{\partial y} e^{-(x^2+y^2)/2} = -2ye^{-(x^2+y^2)/2} \tag{5}$$

We can easily express impulse response of any angle of $h^\theta(x,y)$ by using basis functions given in Equation (4-5), as follows;

$$h^\theta(x,y) = \cos(\theta) \cdot h^0(x,y) + \sin(\theta) \cdot h^{90}(x,y)\ . \tag{6}$$

Thus any directed impulse response of any input image can be found by Equation 6, as a linear combination of basis functions (4) and (5). In Figure 2, the input-output relations of synthetic examples are given for $\theta = 30^0, 135^0$ degrees using Equations (7-8).

$$h^{30}(x,y) = \cos(30) \cdot h^0(x,y) + \sin(30) \cdot h^{90}(x,y) = \frac{\sqrt{3}}{2} \cdot h^0(x,y) + \frac{1}{2} \cdot h^{90}(x,y) \tag{7}$$

$$h^{135}(x,y) = \cos(135) \cdot h^0(x,y) + \sin(135) \cdot h^{90}(x,y) = -\frac{\sqrt{2}}{2} \cdot h^0(x,y) + \frac{\sqrt{2}}{2} \cdot h^{90}(x,y) \tag{8}$$

We can conclude that the dominant effects of the input data can be extracted in the arbitrary chosen angles using steerable filters.

III. APPLICATION OF STEERABLE FILTERS

Here we have applied streerable filters with various angles using equation 6. The anomalies of steerable filter output are condensed at the borders of prismatic structures. In Figure 2b, for the steering angle of 0^0, anomalies occur at in Southern and Northern regions, and they are perpendicular to each other. For 90^0, the anomalies are observed in Southern and Northern regions of these prisms as in Figure 2c to 2d. For 90^0, the anomaly coordinates are just opposite of 0^0 (Figure 2b). In the other arbitrary angles, anomalies are obtained at the corner and borders in the direction of the angles as in Figures 2b-2f. In Figure 2f, the 180^0 steerable filter output seems similar to 0^0.

IV. APPLICATION OF STEERABLE FILTERS FOR REAL DATA

In Bouguer anomaly map of Hatay (Figure 3), -35 mgal contour values are observed around Amik field. Especially on Amanos Mountains contour values reach up to 80 mgal as going to West. The gravity anomaly map of the region seems simple which does not suit the tectonic information's. In Figure 3, DSF is not observed clearly, since there is alluvial covering the fault [15]. But the effect of the western side of DSF seems to be more clearly observed. Thus we decide to apply Steerable filters approach to the Bouguer gravity anomaly map.

In Hatay, Amik area is Pliyo-Kuvaterner with 30 km length [16]. The force forming the fault has also affected the sedimentary rocks, which lie on the West and East of the fault with 90 degrees angle [17]. DSF is more effective in Syria than in Turkey since it is covered by Amik plane composed of alluvial in Turkey [18]. West graben fault is the region of Kahramanmaras and Kirikhan and surrounded by East of Amonos Mountains and vertical shift is dominant.

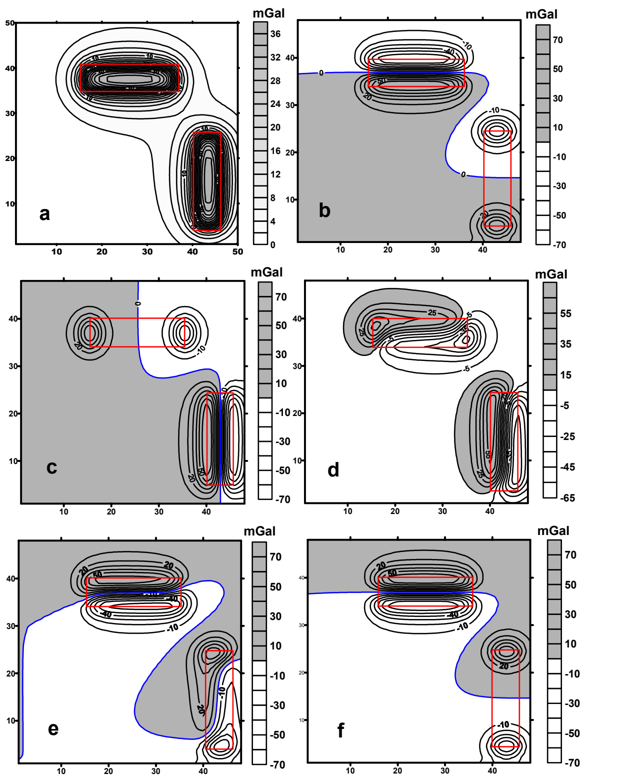

Figure 2. Two perpendicular vertical prism model (in dashed lines) a. Gravity anomaly map. b. Steerable filter output for the input data of gravity anomaly map in Figure 2a with 0^0 arbitrary angle c. with 90^0 d. with 120^0 e. with 160^0 f. with 180^0

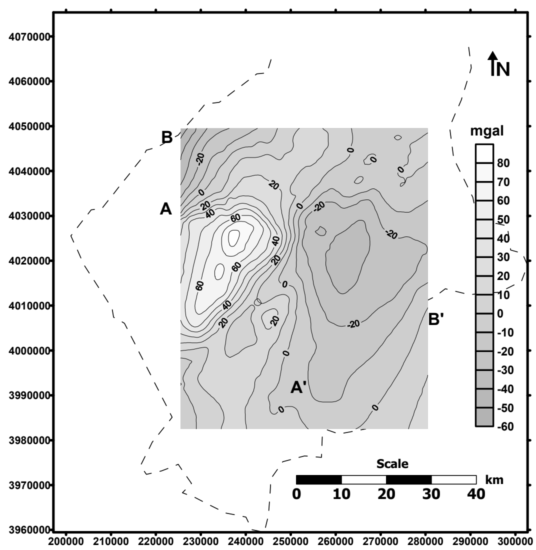

Figure 3. The Bouguer anomaly of Hatay. (The original map is obtained from Turkish Petroleum Cooperation (TPAO)).

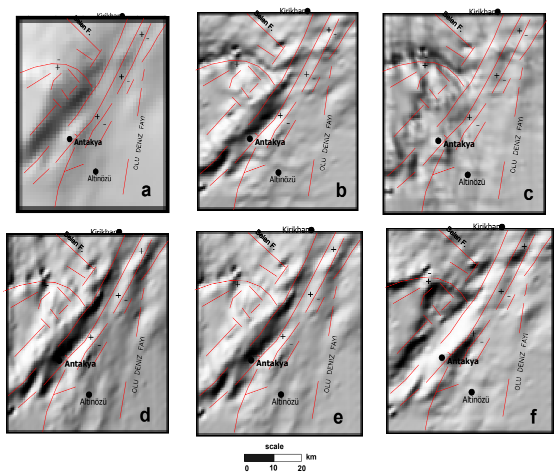

Figure 4. Hatay Region. a. Gravity anomaly map with embossed image. b. Steerable filter outputs with 0^o c. with 40^o d. with 110^o e. with 120^o f. with 160^0

V. CONCLUSION

Steerable filters are used rather frequently for edge detection of images in various directions in Electronics engineering. In this paper we use steerable filters for reveal geophisical problems. This method is applied to gravity anomaly maps formed by prisms that produced from synthetic data (Figure 2). When successful results are obtained then applied to Hatay region. All datas of region are evaluated together while exposing the complicated tectonic structre. For example, Dead Sea Fault (DSF) could not be observed in topography, surface geology and gravity anomalies because of young alluviums. This fault is determined clearly from steerable filters outputs with 90^o and 110^o (Figure 4c and d) and also East Anatolia Fault Zone in figure 4a, d and e. The faults are between 110^o - 120^o angles in the region. Belen Fault and just south of it, there is stronger fault effect that is determined from steerabel filters outputs with 40^o (Figure 4c). As a result of this study, the steerable filter should be used in direction that is close to dominate faults is more efficient to obtaine the faults if the region has a complicated tectonic structure.

CONTRIBUTIONS

We thank Turkish Petroleum Cooperation (TPAO) and for their gravity data. Research Institute of Istanbul University supported this work with the project number 139/20082003.

REFERENCES

1. Freeman W. T. Ve Adelson E. H., 1991. The design and use of steerable filters, IEEE Trans. On Patt. Anl. And Machine Intell, 13, 891-906.

2. Laine A. F. ve Chang C. M., 1995. De-noising via wavelet transforms using steerable filters, Proc. IEEE Int. Sym. On Circuits and Systems, 3, 1956-1959.

3. Özmen A., 2001. Hücresel Yapay Sinir Ağları ve Görüntü İşleme Uygulamaları, İ.Ü. Fen Bilimleri Enstitüsü Doktora Tezi, İstanbul.

4. Davis, A., Murshak, A., Wiscombe, W. 1994. Wavelet-base multi-fractal analysis of non-stationary and/or intermittent geophysical signals. In: Wavelets in Geophysical (eds) E. Foufoula Georgiou and P. Kumar, 249-298. Academic Press, Inc.

5. Chakraborty, A., Okaya, D. 1995. Frequency-time decomposition of seismic data using the wavelet transform-based methods. Geophysics. 60: 1906-1916.

6. Fedi, M., Quata, T., 1998. Wavelet Analysis for the regional-residual and local seperstion at potential field anomalies. Geophys. Prospect. 46: 507-525.

7. Hornby, P., Boschetti, F., Horovitz, F.G. 1999. Analysis of potential field data in the wavelet domain, Geophys. J. Internat. 137, 175-196.

8. Ridsdill-Smith, T.A., Dentith, M. C. 1999. The wavelet transform in aeromagnetic processing, Geophysics. 64: 1003-1013.

9. Holden, D. J., Archıbald, N. J., Boschettı, F., Jessell, m.w. 2000. Inferring Geological Structures using Wavelet-Based multiscale edge analysis and forward models. Explorationa Geophysics. 31: 67-71.

10. Boschetti, F., Hornby, P., Horowitz, F. G. 2001. Wavelet based inversion of gravity data. Exploration Geophysics. 32: 48-55.

11. Ucan, O. N., Seker, S., Albora, A. M., Ozmen, A. 2000. Separation of Magnetic Field in Geophysical Studies Using 2-D Multi Resolution Wavelet Analysis Approach. J. Balkan Geophys. Soc. 3: 53-58.

12. Ucan, O. N., Albora A. M., Hisarlı, Z. M. 2001. Comments on the Gravity and Magnetic Anomalies of Saros Bay using Wavelet approach. Mar. Geophys. Res. 22: 251-264.

13. Fedi, M., Florio, G. 2003. Decorrugation and removal of directional trends of magnetic fields by the wavelet transform: application to archaeological areas. Geophys. Prospect. 51: 261-272.

14. Albora, A. M., Hisarlı, Z. M., Ucan, O. N. 2004. Application of Wavelet Transform to Magnetic Data Due to Ruins of Hittite Civilization in Turkey. Pure Applied Geophys. 161: 907-930

15. Albora A. M., 1998, Hatay bölgesi Gravite yoğunluk dağılımının araştırılması, İ.Ü. Fen Bilimleri Enstitüsü, Doktora tezi, İstanbul.

16. Perincek, D., Cemen, I. 1990. The structural relationship between the East Anatolian Fault and Dead Sea Fault zones in southern Turkey. Tectonophsics. 172: 331-340

17. Yurur, M. T., Chorowicz, J. 1998. Recent volcanism, tectonics and plate kinematics near the junction of the African, Arabian and Anatolian plates in the eastern Mediterranean J. Volcanol. Geoth. Res. 85: 1-15.

18. Hisarlı Z.M., Albora A. M. ve Uçan O. N., 2001. Hatay Bölgesinin Gravite Anomali Haritasından Yararlanarak Bölgenin Tektonik Yapısının Yorumu, Türkiye 14. Jeofizik Kurultayı ve Sergisi, 8-11 Ekim Ankara.